

# Tunable planar Josephson junctions driven by time-dependent spin-orbit coupling

David Monroe,<sup>1</sup> Mohammad Alidoust,<sup>2</sup> and Igor Žutić<sup>1</sup>

<sup>1</sup>University at Buffalo, State University of New York, Buffalo, New York 14260-1500, USA

<sup>2</sup>Department of Physics, Norwegian University of Science and Technology, N-7491 Trondheim, Norway

(Dated: Received 18 April 2022; revised 10 July 2022; accepted 2 August 2022; published 15 September 2022)

The integration of conventional superconductors with common III-V semiconductors provides a versatile platform to implement tunable Josephson junctions (JJs) and their applications. We propose that with gate-controlled time-dependent spin-orbit coupling, it is possible to strongly modify the current-phase relations and Josephson energy and provide a mechanism to drive the JJ dynamics, even in the absence of any bias current. We show that the transition between stable phases is realized with a simple linear change in the strength of the spin-orbit coupling, while the transition rate can exceed the gate-induced electric field gigahertz changes by an order of magnitude. The resulting interplay between the constant effective magnetic field and changing spin-orbit coupling has direct implications for superconducting spintronics, the control of Majorana bound states, and emerging qubits. We argue that topological superconductivity, sought for fault-tolerant quantum computing, offers simpler applications in superconducting electronics and spintronics.

DOI: [10.1103/PhysRevApplied.18.L031001](https://doi.org/10.1103/PhysRevApplied.18.L031001)

In the push to implement beyond-CMOS applications, Josephson junctions (JJs) have found their broad use due to their high-speed switching, low-power dissipation, and intrinsic nonlinearities[1, 2]. In addition to the well-established role of JJs as the key elements for superconducting electronics and superconducting qubits[1–6], there is a growing interest in tailoring their spin-dependent properties to enable dissipationless spin currents, cryogenic memory[7–14], and fault-tolerant quantum computing[15–22]. The role of spin-orbit coupling (SOC) has been extensively studied in the normal-state properties and recognized for its importance in spintronics[23–25]. However, the superconducting analogs of the SOC-related effects remain to be understood. They might even be important when their normal-state counterparts are negligibly small[26–32]. Motivated by the recent progress in gate-controlled SOC in planar JJs based on a two-dimensional electron gas (2DEG)[33–35], we reveal how time-dependent SOC tunes many of their key properties and offers an unexplored mechanism to drive JJs.

A common description of a JJ circuit, is given by a Josephson element, resistor, and capacitor connected in parallel, using the resistively and capacitively shunted junction (RSCJ)[1] model. The bias current through the junction,  $i$ , is the sum of the supercurrent and the quasiparticle current flowing in the resistor and capacitor. The supercurrent is usually assumed as  $I(\varphi) = I_c \sin(\varphi + \varphi_0)$ , where  $I_c$  is the maximum supercurrent,  $\varphi$  is the phase difference between the superconducting regions, and the anomalous phase,  $\varphi_0 \neq 0, \pi$ , arises from the broken time-reversal and inversion symmetries[37–43].

For a ballistic JJ depicted in Fig. 1(a), the interplay between SOC and the effective Zeeman field  $\mathbf{h}$ , yields a more complex current-phase relation (CPR) than  $I(\varphi)$

given above, such that for a generalized RSCJ model

$$d^2\varphi/d\tau^2 + (d\varphi/d\tau)/\sqrt{\beta_c} + I(\varphi, \mu, \mathbf{h}, \alpha)/I_c = i/I_c, \quad (1)$$

where  $\tau = \omega_p t$  is a dimensionless time, expressed using the JJ plasma frequency,  $\omega_p = \sqrt{2\pi I_c / \Phi_0 C}$ ,  $\Phi_0 = h/2e$  is the magnetic flux quantum, and  $C$  is the capacitance. The damping of this nonlinear oscillator is characterized by the Stewart-McCumber parameter,  $\beta_c = 2\pi I_c C R^2 / \Phi_0$ , where  $R$  is the resistance[44, 45] and  $Q = \sqrt{\beta_c}$  is the quality factor. The generalized CPR can be modified by the chemical potential  $\mu$ , and  $\mathbf{h}$ , arising from the applied magnetic field or magnetic proximity effect[46]. Since  $h_z$  does not induce  $\varphi_0$ [47, 48] and only produces CPR reversals, we focus on  $h_z = 0$  [Fig. 1(a)]. The CPR can also be tuned by the Rashba SOC, illustrated in Fig. 1(a), which is parametrized by its strength  $\alpha$ , in the Hamiltonian,  $H_{so} = \alpha(\boldsymbol{\sigma} \times \mathbf{p}) \cdot \hat{\mathbf{z}}$ . Here,  $\boldsymbol{\sigma}$  is the Pauli matrix vector, and  $\mathbf{p}$  is the in-plane momentum, for 2DEG with the inversion symmetry broken along the  $z$ -direction[49].

While quasistatic gate-tunable changes in SOC and  $\varphi_0$  have been demonstrated in 2DEG-based JJs[33, 34], the implications of dynamically tuned SOC on the CPR remain unexplored. For a conventional CPR without any  $\varphi_0$ , Eq. (1) has a mechanical analog with a driven and damped pendulum, in which  $\varphi$  becomes the displacement angle[44, 45]. A JJ driven by  $i$  is equivalent to the pendulum displaced by an external torque from its stable equilibrium, determined by the gravitational acceleration  $\mathbf{g}$ , while  $\omega_p$  determines the oscillation frequency around a stable equilibrium point[1].

Instead of using  $i$ , Fig. 1(b) suggests an entirely different way to drive the pendulum: By changing the orientation of the effective  $\mathbf{g}'$  and the new equilibrium, resulting from the interplay of the static  $\mathbf{h}$  and time-dependent  $\alpha$ .

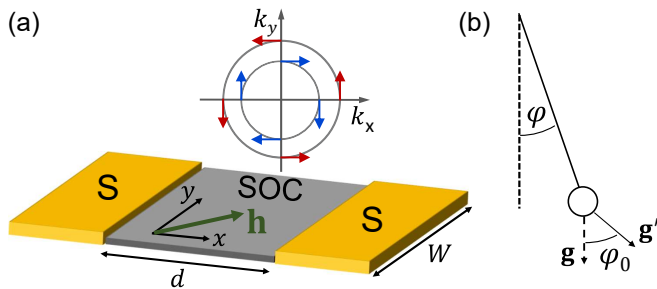


FIG. 1. (a) A schematic of the Josephson junction (JJ). Two  $s$ -wave superconductors ( $S$ ), are separated by the middle region which hosts the Rashba spin-orbit coupling (SOC), with depicted  $\mathbf{k}$ -space spin-orbit fields, and an effective Zeeman field,  $\mathbf{h}$ . (b) A mechanical pendulum model of the JJ. The displacement angle  $\varphi$  is analogous to the superconducting phase difference and  $\mathbf{g}$  is the gravitational acceleration for vanishing SOC and  $\mathbf{h}$ . The pendulum is driven by changing the effective  $\mathbf{g}'$ , an interplay between  $\mathbf{h}$  and time-dependent SOC. This yields a tunable current-phase relation and an anomalous phase,  $\varphi_0$ , equivalent to the equilibrium of the displaced pendulum.

With JJ advances and gate changes exceeding the gigahertz range[3], there is a tantalizing prospect for dynamically controlled CPR by time-dependent SOC. Unlike assuming a specific relation,  $I(\varphi) = I_c \sin(\varphi + \varphi_0)$ , the CPR can have a more general and anharmonic form which should be obtained microscopically. To this end, a single-particle Hamiltonian,  $H(\mathbf{p}) = \mathbf{p}^2/2m^* + \boldsymbol{\sigma} \cdot \mathbf{h} + H_{\text{so}}(\mathbf{p})$ , where  $m^*$  is the effective mass, can be used to solve a BCS model of superconductivity, given by the effective Hamiltonian

$$\mathcal{H}(\mathbf{p}) = \begin{pmatrix} H(\mathbf{p}) - \mu\hat{1} & \hat{\Delta} \\ \hat{\Delta}^\dagger & -H^\dagger(-\mathbf{p}) + \mu\hat{1} \end{pmatrix}, \quad (2)$$

where  $\hat{\Delta}$  is a  $2 \times 2$  superconducting gap in spin space[47].

After diagonalizing the resulting Bogoliubov-de Gennes equations,  $\mathcal{H}\hat{\psi} = E\hat{\psi}$ , where  $\hat{\psi}$  is the four-component wave function for quasiparticle states with energy  $E$ , we match the wave functions and generalized velocities at interfaces ( $x = 0, d$ ), shown in Fig. 1(a). This allows us to obtain the ground-state JJ energy  $E_{\text{GS}}$ , together with the corresponding CPR, using charge conservation and the quantum definition of current[47]. The CPR is related to the JJ energy:  $I(\varphi) \propto \partial E_{\text{GS}}/\partial \varphi$ [50].

Our numerical findings are illustrated for the JJ depicted in Fig. 1(a). The normal region ( $N$ ) has a length  $L = 0.3\xi_S$  and a width  $W = 10L$ , such that lengths are normalized by  $\xi_S = \hbar/\sqrt{2m^*\Delta}$ , where  $\Delta$  is the superconducting gap in  $S$ . The energies are normalized by  $\Delta$  and the supercurrent  $I_0 = 2|e\Delta|/\hbar$ , where  $e$  is the electron charge and  $|e\Delta|/\hbar$  is the maximum supercurrent in a single-channel short  $S$ - $N$ - $S$  JJ[50].

To explore the tunability of CPRs and JJ energies with SOC, we focus on the parameters for high-quality epitaxial InAs-Al based JJs,  $\Delta_{\text{Al}} = 0.2 \text{ meV}$ , with a  $g$ -

factor of 10 for InAs, while its  $m^*$  is 0.03 times the electron mass[33, 34]. In these JJs the gate control of Rashba SOC and thus its magnitude in the range  $\alpha \in (0, 180 \text{ meV}\text{\AA})$  has been demonstrated[33, 34]. In Fig. 2, at  $h_x = (2/3)\Delta \approx 450 \text{ mT}$ , we assume gate control process that primarily changes  $\alpha$ , not  $\mu$ . Experimentally, this could be realized with dual-gate schemes[51] to independently tune the carrier density and the electric field,  $\mathbf{E}$ . However, for a continuous change of  $\alpha$ , we are unaware that even in a static case the calculated CPR and  $E_{\text{GS}}$  are given.

In Fig. 2(a), for  $\mu = \Delta$ , the anharmonic CPR changes significantly with  $\alpha$ . There is a competition between  $\sin \varphi$  and the next harmonic,  $\sin 2\varphi$ , resulting in  $I(-\varphi) = -I(\varphi)$ . However, there is no spontaneous current,  $I(\varphi = 0) \equiv 0$ , only  $I_c$  reversal with  $\alpha$ . Such a continuous and symmetric  $0$ - $\pi$  transition is well studied without SOC in  $S$ /ferromagnet/ $S$  JJs due to the changes in the effective magnetization, temperature, or the thickness of the magnetic region[52–60]. The corresponding JJ energy landscape in Fig. 2(b), shifted such that its overall minimum value is 0, corroborates this SOC evolution. By increasing  $\alpha$  from 0 to  $200 \text{ meV}\text{\AA}$ , the minimum in  $E_{\text{GS}}$  changes from  $\varphi = 0$  to  $\pi$ , and then goes back to 0. A gray trace indicates that by increasing  $\alpha$  in a smaller range, the JJ minimum can transition from  $\varphi = 0$  to approximately  $\pi/2$ .

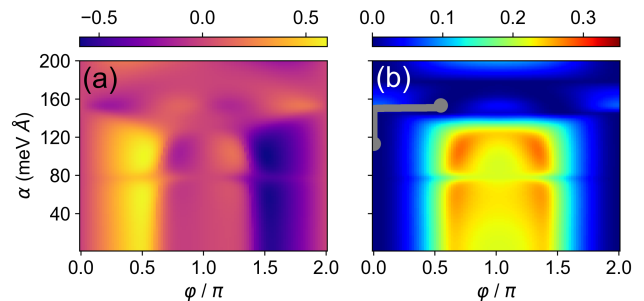


FIG. 2. (a) The evolution of (a) JJ CPR, normalized by  $2|e\Delta|/\hbar$ , and (b) the JJ energy, normalized by  $\Delta$ , as a function of the phase  $\varphi$  and the Rashba SOC,  $\alpha$ , for chemical potential  $\mu = \Delta$  and effective in-plane magnetic field,  $h_x = (2/3)\Delta$ . The gray curve in (b) denotes the JJ transition from  $\varphi = 0$  to  $\approx \pi/2$  for a linear increase in  $\alpha$  from 112 to 152  $\text{meV}\text{\AA}$ .

While we use an exact (complete) CPR with its anharmonicities, their prior descriptions have often relied on an approximate simple harmonic expansion ( $\sin n\varphi, \cos n\varphi$ )[61, 62]. However, this approach is not very efficient with SOC. Instead, it is better to use a compact form where only a small number of terms gives a more accurate description[47]

$$I(\varphi, \mu, \mathbf{h}, \alpha) \approx \sum_{n=1}^N \sum_{\sigma=\pm} \frac{I_n^\sigma \sin(n\varphi + \varphi_{0n}^\sigma)}{\sqrt{1 - \tau_n^\sigma \sin^2(n\varphi/2 + \varphi_{0n}^\sigma/2)}}, \quad (3)$$

where  $\tau_n^\sigma$  is the JJ transparency for spin channel  $\sigma$  and the phase shifts  $\varphi_{0n}$  are additional fitting parameters. This description includes the anomalous Josephson effect  $I(\varphi = 0) \neq 0$ , revisited in JJ diode effects[63–67]. For a simple picture of a single anomalous phase[47, 48].

$$\varphi_0 \propto h_y \alpha^3, \quad (4)$$

therefore vanishing in Fig. 2, where  $\mathbf{h} = h_x \hat{x}$ .

A quasistatic gate-controlled SOC suggests that more important opportunities are available using fast gate changes, compatible with the advances in JJ circuits[3]. However, the implications of gigahertz changes in SOC and a different mechanism to drive JJ, as sketched in Fig. 1(b), remain unexplored. To obtain the resulting JJ dynamics we use Eq. (1) with  $i \equiv 0$ , where the driving arises from  $\alpha = \alpha(t)$ , viewed as a time-dependent effective  $\mathbf{g}'$ .

Some guidance as to what to expect for JJ dynamics can be given from the InAs-Al samples, where, in addition to the previous range of  $\alpha$ ,  $I_c \sim 4 \mu\text{A}$ ,  $R \sim 100 \Omega$ , and  $C \sim 15 \text{fF}$ , leading to  $\omega_p \sim 900 \text{GHz}$  and the damping  $\beta_c \sim 1$ , which is also suitable for the rapid single-flux quantum (RSFQ) applications[1, 4]. We keep  $h_x = (2/3)\Delta$ .

The JJ dynamics are driven by a simple linear variation of  $\alpha(t)$  from the gate-controlled  $\mathbf{E}$ , as shown in Fig. 3(a). We first consider in Fig. 3(b) the reduction of  $\omega_p$ , from 1000 GHz (similar to InAs-Al JJs[33]) to 10 GHz (much faster than the  $\alpha(t)$  variation), at  $\beta_c = 1$ . The results reveal a strong delay in the onset in the  $\varphi = 0$  to approximately  $\pi/2$  transition, which is indicated from the static picture in Fig. 2(b). Simultaneously, the time for the  $\varphi = 0$  to approximately  $\pi/2$  transition is increased by an order of magnitude.

We next examine, in the inset of Fig. 3(b), the influence of reducing  $\beta_c$  from the underdamped and critical ( $\beta_c = 10$  and 1) to the overdamped ( $\beta_c = 0.1$ ) regime, at  $\omega_p = 1000 \text{GHz}$ . In addition to the phase-oscillation damping, consistent with the pendulum model in Fig. 1(b), we also see a delay in the  $\varphi = 0$  to approximately  $\pi/2$  transition and its growth, the trends noted from reducing  $\omega_p$ .

Finally, in Fig. 3(c), the  $\varphi = 0$  to approximately  $\pi/2$  transition occurs first for the slower  $\alpha(t)$  variation, but takes approximately the same time as the faster gigahertz  $\alpha(t)$  variation. This is encouraging for various applications, since (i)  $\mathbf{E}$  control of SOC allows tailoring of the onset of the transition between different states, (ii) a high-frequency switching between different equilibrium states and driving JJs is not limited by the characteristic times for the  $\mathbf{E}$  variation.  $\alpha(t)$  changes at 0.2 GHz give an order-of-magnitude faster transition between the stable phases.

While the  $\mathbf{E}$  control of  $\alpha$  and the evolution of the  $E_{\text{GS}}$  minima in Fig. 2 largely determine the JJ dynamics in Fig. 3, it helps to identify other opportunities for SOC-driven JJs. In Fig. 4, we consider  $\omega_p = 10 \text{GHz}$  and a triangularlike  $\alpha(t)$  at  $\mu = 10\Delta$ . For an underdamped regime,  $\beta_c = 10$ , the pendulum analogy from Fig. 1(b)

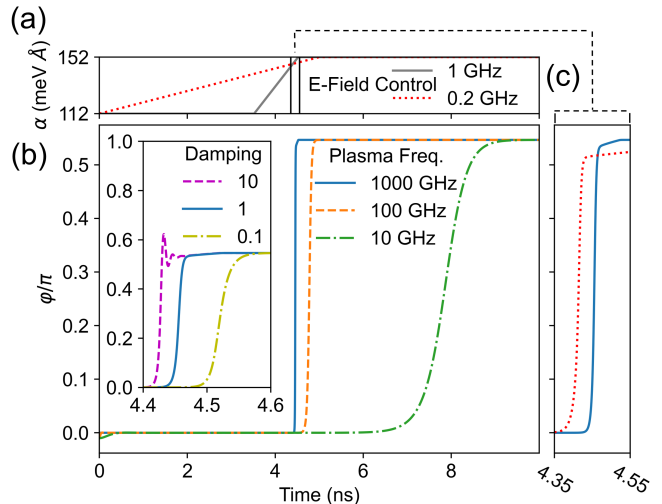


FIG. 3. (a) A time-dependent Rashba SOC,  $\alpha$ , controlled by the  $\mathbf{E}$ -field, changing at 0.2 GHz and 1 GHz, and also used in (b). (b) The time-dependent phase for different plasma frequencies,  $\omega_p$ , at damping,  $\beta_c = 1$ , and for different  $\beta_c$  at  $\omega_p = 1000 \text{GHz}$  (inset). (c) An enlarged region for  $\varphi = 0$  to approximately  $\pi/2$  transition at 0.2 GHz (1 GHz) dotted (solid) changes in  $\alpha$  from (a).

explains the phase evolution of the gray trajectory from Fig. 4(a), also reproduced in Fig. 4(c). By increasing  $\alpha$  to the maximum at 192 meVÅ, the pendulum is at an unstable position and will swing toward the  $\varphi = 0$  minimum (equivalently shown as  $\varphi = 2\pi$ ), implying that  $\mathbf{g}'$  points vertically down. With small damping (gray trajectory), the pendulum passes the equilibrium point, even when, with  $\alpha < 80 \text{meVÅ}$ , the equilibrium and the overall minimum shift to  $\varphi = \pi$ , with  $\mathbf{g}'$  vertically up. Eventually, with damping it reaches the  $\varphi = \pi$  minimum.

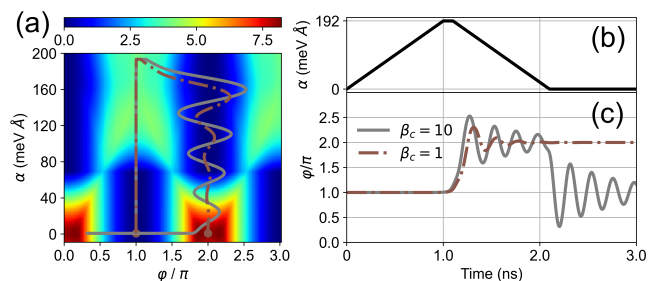


FIG. 4. (a) The JJ energy evolution with  $\varphi$  and  $\alpha$  at  $\mu = 10\Delta$ ,  $h_x = (2/3)\Delta$ . The gray (brown) curve shows the energy variation for  $\beta_c = 10$  ( $\beta_c = 1$ ) starting at  $\varphi = \pi$  and  $\alpha = 0$ , for changing  $\alpha$ , as given in (b). (c) The corresponding time-dependent  $\varphi$  confirms the decay to different final phase states.

For critical damping, with the same starting point [see also Fig. 4(c)], the brown trajectory reveals a very different evolution with  $\alpha$ . Instead at the overall  $E_{\text{GS}}$  minimum  $\varphi = \pi$ , for  $\alpha = 0$ , the phase is locked at the local minimum  $\varphi = 0$ . With a stronger damping, the  $\varphi$  oscill-

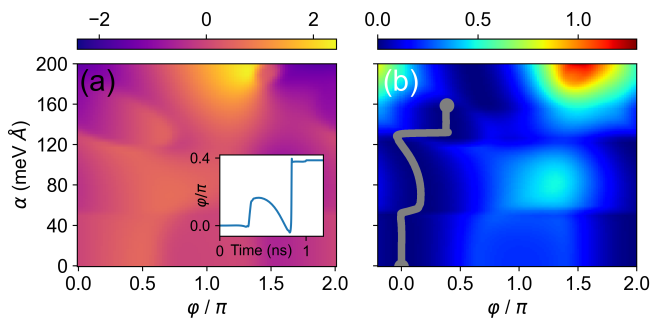


FIG. 5. The evolution of (a) JJ CPR and (b) the JJ energy with  $\varphi$  and  $\alpha$ , for  $\mu = \Delta$  and  $h_y = (2/3)\Delta$ , rotated by  $\pi/2$  from Fig. 2. An anharmonic CPR breaks the  $I(-\varphi) = -I(\varphi)$  symmetry in (a) and the corresponding anomalous phase,  $\varphi_0$ , increases with  $\alpha$  in (b). The inset in (a) shows  $\varphi(t)$  for  $\omega_p = 1000$  GHz,  $\beta_c = 1$  with a linearly increasing  $\alpha$  from 0 to 160 meVÅ over 1 ns, which is then held at a maximum, with its JJ energy path in (b).

lations are insufficient to overcome the SOC-dependent barrier which, for  $\alpha = 0$ , separates the local minimum at  $\varphi = \pi$  from the global one at  $\varphi = 2\pi$ . The tunability of the SOC-controlled energy landscape alone does not fully determine the generalized CPRs. The influence of the JJ circuit parameters can enable different  $\varphi$  transitions.

In the above discussion, the tunability of CPRs and  $E_{GS}$  does not exploit the anomalous Josephson effect [37–40, 70], which can be understood in analogy to  $\mathbf{g}'$  pointing sideways and therefore, breaking the symmetry from Figs. 2-4 and  $I(-\varphi) \neq -I(\varphi)$ . This situation can be simply realized by rotating  $\mathbf{h}$  along the  $y$  axis, while we retain all the other parameters from Fig. 2(a). The resulting CPR in Fig. 5(a) confirms that the JJ supercurrent is driven not only by  $\varphi$  but also by  $\varphi_0$ , which is responsible for the stated symmetry breaking and, equivalently, the tilted  $\mathbf{g}'$ . As for SOC cubic in  $\mathbf{k}$  [47], there is a strong anharmonic behavior and the expected diode effect, where the sign and magnitude of the supercurrent depend on the polarity of the applied bias [34].

The implications of the combined broken time-reversal and inversion symmetries, responsible for the anomalous Josephson effect, are further illustrated in Fig. 5(b), which shows the SOC-tunable  $E_{GS}$ , single valued for the gray path, and leading to the time-dependent diode effect. This behavior is qualitatively different from the doubly degenerate  $\varphi_0$  state in Fig. 2(b), which results from the second-harmonic generation in the CPR.

Even with a moderate  $h_y \approx 450$  mT for InAs based JJs, with increasing  $\alpha(t)$  we see an evolution of the single global minimum and thus the changes in the corresponding values of  $\varphi_0$  from  $\varphi = 0$  to approximately  $3\pi/4$ , in good agreement with the measured values [33]. This suggests that at a larger  $\mathbf{h}$ , for example, in In(As,Sb) with a much larger  $g$  factor [35], it may be possible to fully control the tilt angle of  $\mathbf{g}'$  and simply swap between 0 and  $\pi$  states in JJs, further controlling how the JJ dynamics

are driven.

The same geometry in Al-InAs JJs at a larger  $h_y$  has been experimentally shown to also support topological superconductivity [34]. This is important for several reasons, beyond hosting Majorana bound states [16]. The resulting topological superconductivity is associated with equal-spin  $p$ -wave superconductivity which could offer gate-controlled dissipationless spin currents, a key element for superconducting spintronics [7, 8]. Such spin-triplet supercurrents could be extended over a long range [71] and could overcome the usual competition between superconductivity and ferromagnetism. A transition to topological superconductivity is accompanied by an extra phase jump, of approximately  $\pi$  [72, 73]. Such a  $\pi$  jump in Al-InAs JJs has been observed at  $h_y \approx 600$  mT [34], an effective field about 25 times smaller, than expected for the  $0-\pi$  transition

$$B_{0-\pi} = (\pi/2)\hbar v_F / (g\mu_B L), \quad (5)$$

for a spin-polarized system in the absence of SOC [74], where  $v_F$  is the Fermi velocity,  $\mu_B$  the Bohr magneton, and  $L$  the JJ length. Therefore, SOC plays a crucial role in understanding various transitions and, at larger  $h_y$ , the range of an effective  $\varphi_0$  could exceed  $2\pi$  [34] and support  $2\pi$  pendulum rotation from Fig. 1(b), as used in RSFQ logic and memory [1, 4]. Therefore, in addition to the prospect of fault-tolerant quantum computing, the search for topological superconductivity also offers a promising platform for superconducting electronics and spintronics.

Without previous studies on SOC-driven JJ dynamics, we focus on a simple model and do not consider time-dependent magnetic fields [75] or noise [76]. A more general description could simultaneously include the role of changing  $\mu$  and other SOC forms, linear and cubic in  $\mathbf{k}$ , shown to give different routes to topological superconductivity and control of Majorana states [47, 77–79]. However, we expect that our focus only on linearized Rashba SOC, easily tunable by  $\mathbf{E}$  field [33, 34], already clarifies its important role in JJ dynamics. With changing SOC, there are further opportunities for gate-controlled Majorana states and the probing of their non-Abelian statistics [80, 81] or an added tunability in the implementation of superconducting qubits [3, 82, 83]. This would extend the previously studied qubit tunability by voltage or flux [3, 84] as well as the use of  $\pi$ -phase states for an improved qubit operation [85, 86].

## ACKNOWLEDGMENTS

We thank Javad Shabani and Tong Zhou for valuable discussions. This work is supported by the National Science Foundation (NSF) Electrical, Communications and Cyber Systems (ECCS) Grant No. 2130845, the U.S. Office of Naval Research (ONR) through Grants No. N000141712793 and MURI No. N000142212764 (D. M.

- 
- [1] F. Tafuri (ed.), *Fundamentals and Frontiers of the Josephson Effect*, (Springer Nature, Cham, 2019).
- [2] M. Siegel and M. Hidaka, Superconductor Digital Electronics, in *Nanoelectronics and Information Technology 3rd Ed.*, edited by R. Wasner (Wiley-VCH, Weinheim, Germany 2012), pp. 421-430.
- [3] P. Krantz, M. Kjaergaard, F. Yan, T. P. Orlando, S. Gustavsson, and W. D. Oliver, A Quantum Engineer's Guide to Superconducting Qubits, *Appl. Phys. Rev.* **6**, 021318 (2019).
- [4] K. K. Likharev and V. K. Semenov, RSFQ Logic/Memory Family: A New Josephson-Junction Technology for Sub-Terahertz-Clock-Frequency Digital Systems, *IEEE Trans. Appl. Supercond.* **1**, 3 (1991).
- [5] D. S. Holmes, A. L. Ripple, and M. A. Manheimer, Energy-Efficient Superconducting Computing-Power Budgets and Requirements, *IEEE Trans. Appl. Supercond.* **23**, 1701610 (2013).
- [6] F. Giazotto, J. T. Peltonen, M. Meschke, and J. P. Pekola, Superconducting quantum interference proximity transistor, *Nat. Phys.* **6**, 254 (2010).
- [7] M. Eschrig, Spin-polarized supercurrents for spintronics: A review of current progress, *Rep. Prog. Phys.* **78**, 104501 (2015).
- [8] J. Linder and J. W. A. Robinson, Superconducting spintronics, *Nat. Phys.* **11**, 307 (2015).
- [9] T. S. Khaire, M. A. Khasawneh, W. P. Pratt, Jr., and N. O. Birge, Observation of Spin-Triplet Superconductivity in Co-Based Josephson Junctions, *Phys. Rev. Lett.* **104**, 137002 (2010).
- [10] N. Banerjee, J. W. A. Robinson, and M. G. Blamire, Reversible control of spin-polarized supercurrents in ferromagnetic Josephson junctions, *Nat. Commun.* **5**, 4771 (2014).
- [11] E. C. Gingrich, B. M. Niedzielski, J. A. Glick, Y. Wang, D. L. Miller, R. Loloee, W. P. Pratt, Jr., and N. O. Birge, Controllable  $0 - \pi$  Josephson junctions containing a ferromagnetic spin valve, *Nat. Phys.* **12**, 564 (2016).
- [12] N. O. Birge and M. Houzet Spin-Singlet and Spin-Triplet Josephson Junctions for Cryogenic Memory, *IEEE Magn. Lett.* **9**, 4509605 (2019).
- [13] A. A. Mazanik, I. R. Rahmonov, A. E. Botha, and Yu. M. Shukrinov, Analytical criteria for magnetization reversal in  $\varphi_0$  Josephson junction, *Phys. Rev. Applied* **14**, 014003 (2020).
- [14] W. Han, S. Maekawa, and X.-C. Xie, Spin current as a probe of quantum materials. *Nat. Mater.* **19**, 139 (2020).
- [15] L. Fu and C. L. Kane, Superconducting Proximity Effect and Majorana Fermions at the Surface of a Topological Insulator, *Phys. Rev. Lett.* **100**, 096407 (2008).
- [16] D. Aasen, M. Hell, R. V. Mishmash, A. Higginbotham, J. Danon, M. Leijnse, T. S. Jespersen, J. A. Folk, C. M. Marcus, K. Flensberg, and J. Alicea, Milestones Toward Majorana-Based Quantum Computing, *Phys. Rev. X* **6**, 031016 (2016).
- [17] K. Laubscher and J. Klinovaja, Majorana bound states in semiconducting nanostructures, *J. Appl. Phys.* **130**, 081101 (2021).
- [18] U. Güngördü and Alexey A. Kovalev, Majorana bound states with chiral magnetic textures, preprint.
- [19] L. P. Rokhinson, X. Liu, and J. K. Furdyna, The fractional a.c. Josephson effect in a semiconductor-superconductor nanowire as a signature of Majorana particles, *Nat. Phys.* **8**, 795 (2012).
- [20] A. Fornieri, A. M. Whiticar, F. Setiawan, E. Portolés, A. C. C. Drachmann, A. Keselman, S. Gronin, C. Thomas, T. Wang, R. Kallaher, G. C. Gardner, E. Berg, M. J. Manfra, A. Stern, C. M. Marcus, and F. Nichele, Evidence of topological superconductivity in planar Josephson junctions, *Nature* **569**, 89 (2019).
- [21] H. Ren, F. Pientka, S. Hart, A. Pierce, M. Kosowsky, L. Lunczer, R. Schlereth, B. Scharf, E. M. Hankiewicz, L. W. Molenkamp, B. I. Halperin, and A. Yacoby, Topological superconductivity in a phase-controlled Josephson junction, *Nature* **569**, 93 (2019).
- [22] M. M. Desjardins, L. C. Contamin, M. R. Delbecq, M. C. Dartiaill, L. E. Bruhat, T. Cubaynes, J. J. Viennot, F. Mallet, S. Rohart, A. Thiaville, A. Cottet, and T. Kontos, Synthetic spin-orbit interaction for Majorana devices, *Nat. Mater.* **18**, 1060 (2019).
- [23] I. Žutić, J. Fabian, and S. Das Sarma, Spintronics: Fundamentals and applications, *Rev. Mod. Phys.* **76**, 323 (2004).
- [24] J. Fabian, A. Matos-Abiague, C. Ertler, P. Stano, and I. Žutić, Semiconductor Spintronics, *Acta Phys. Slov.* **57**, 565 (2007).
- [25] D. Bercioux and P. Lucignano, Quantum transport in Rashba spin-orbit materials: a review, *Rep. Prog. Phys.* **78**, 106001 (2015).
- [26] I. Högl, A. Matos-Abiague, I. Žutić, and J. Fabian, Magnetoanisotropic Andreev Reflection in Ferromagnet/Superconductor, *Phys. Rev. Lett.* **115**, 116601 (2015).
- [27] A. Costa, P. Högl, and J. Fabian Magnetoanisotropic Josephson effect due to interfacial spin-orbit fields in superconductor/ferromagnet/superconductor junctions, *Phys. Rev. B* **95**, 024514 (2017).
- [28] P. Lv, Y.-F. Zhou, N.-X. Yang, and Q.-F. Sun, Magnetoanisotropic spin-triplet Andreev reflection in ferromagnet-Ising superconductor junctions, *Phys. Rev. B* **97**, 144501 (2018).
- [29] I. Martínez, P. Högl, C. González-Ruano, J. Pedro Cascales, C. Tiusan, Y. Lu, M. Hehn, A. Matos-Abiague, J. Fabian, I. Žutić, and F. G. Aliev, Interfacial Spin-Orbit Coupling: A Platform for Superconducting Spintronics, *Phys. Rev. Applied* **13**, 014030 (2020).
- [30] T. Vezin, C. Shen, J. E. Han, *et al.*, Enhanced spin-triplet pairing in magnetic junctions with *s*-wave superconductors, *Phys. Rev. B* **101**, 014515 (2020).
- [31] C. González-Ruano, L. G. Johnsen, D. Caso, *et al.*, Superconductivity-induced change in magnetic anisotropy in epitaxial ferromagnet-superconductor hybrids with spin-orbit interaction, *Phys. Rev. B* **102**, 020405(R) (2020).
- [32] R. Cai, Y. Yao, P. Lv, *et al.*, Evidence for anisotropic spin-triplet Andreev reflection at the 2D van der Waals

- ferromagnet/superconductor interface, *Nat. Commun.* **12**, 6725 (2021).
- [33] W. Mayer, M. C. Dartiailh, J. Yuan, K. S. Wickramasinghe, E. Rossi, and J. Shabani, Gate controlled anomalous phase shift in Al/InAs Josephson junctions, *Nat. Commun.* **11**, 21 (2020).
- [34] M. Dartiailh, W. Mayer, J. Yuan, K. Wickramasinghe, A. Matos-Abiague, I. Žutić, and J. Shabani, Phase Signature of Topological Transition in Josephson Junctions, *Phys. Rev. Lett.* **126**, 036802, (2021).
- [35] An even larger Rashba SOC is possible in other JJs. [36]
- [36] W. Mayer, W. F. Schiela, J. Yuan, M. Hatefipour, W. L. Sarney, S. P. Svensson, A. C. Leff, T. Campos, K. S. Wickramasinghe, M. C. Dartiailh, I. Žutić, and J. Shabani, Superconducting Proximity Effect in InAsSb Surface Quantum Wells with In-Situ Al Contact, *ACS Appl. Electron. Mater.* **2**, 2351(2020).
- [37] A. A. Reynoso, G. Usaj, C. A. Balseiro, D. Feinberg, and M. Avignon, Anomalous Josephson Current in Junctions with Spin Polarizing Quantum Point Contacts, *Phys. Rev. Lett.* **101**, 107001 (2008).
- [38] A. Buzdin, Direct Coupling Between Magnetism and Superconducting Current in the Josephson  $\varphi_0$  Junction, *Phys. Rev. Lett.* **101**, 107005 (2008).
- [39] F. Konschelle and A. Buzdin, Magnetic Moment Manipulation by a Josephson Current, *Phys. Rev. Lett.* **102**, 017001 (2009).
- [40] H. Sickinger, A. Lipman, M. Weides, R. G. Mints, H. Kohlstedt, D. Koelle, R. Kleiner, and E. Goldobin, Experimental Evidence of a  $\varphi$  Josephson Junction, *Phys. Rev. Lett.* **109**, 107002 (2012).
- [41] E. Strambini, A. Iorio, O. Durante, R. Citro, C. Sanz-Fernández, C. Guarcello, I. V. Tokatly, A. Braggio, M. Rocci, N. Ligato, V. Zannier, L. Sorba, F. S. Bergeret, and F. Giazotto, A Josephson phase battery, *Nat. Nanotechnol.* **15**, 656 (2020).
- [42] Yu. M. Shukrinov, Anomalous Josephson effect, *Phys.-Usp.* **65**, 317 (2022).
- [43] I. I. Soloviev, V. I. Ruzhickiy, S. V. Bakurskiy, N. V. Klenov, M. Yu. Kupriyanov, A. A. Golubov, O. V. Skryabina, and V. S. Stolyarov, Superconducting Circuits without Inductors Based on Bistable Josephson Junctions, *Phys. Rev. Applied* **16**, 014052 (2021).
- [44] W. C. Stewart, Current-Voltage Characteristics of Josephson junctions, *Appl. Phys. Lett.* **12**, 277 (1968).
- [45] D. E. McCumber, Effect of ac Impedance on dc Voltage-Current Characteristics of Superconductor Weak-Link Junctions, *J. Appl. Phys.* **39**, 3113 (1968).
- [46] I. Žutić, A. Matos-Abiague, B. Scharf, H. Dery, and K. Belashchenko, Proximitized materials, *Mater. Today* **22**, 85 (2019).
- [47] M. Alidoust, C. Shen, and I. Žutić, Cubic spin-orbit coupling and anomalous Josephson effect in planar junctions, *Phys. Rev. B* **103**, L060503 (2021).
- [48] M. Alidoust, Critical supercurrent and  $\varphi_0$  state for probing a persistent spin helix, *Phys. Rev. B* **101**, 155123 (2020).
- [49] Y. A. Bychkov and E. I. Rashba, Properties of a 2D electron gas with lifted spectral degeneracy, *Pis'ma Zh. Eksp. Teor. Fiz.* **39**, 66 (1984) [*JETP Lett.* **39**, 78 (1984)].
- [50] A. Zagoskin, *Quantum Theory of Many-Body Systems*, 2nd ed. (Springer, New York, 2014).
- [51] D. Van Tuan, B. Scharf, Z. Wang, J. Shan, K.-F. Mak, I. Žutić, and H. Dery, Probing many-body interactions in monolayer transition-metal dichalcogenides, *Phys. Rev. B* **99**, 085301 (2019).
- [52] T. Kontos, M. Aprili, J. Lesueur, F. Genêt, B. Stephanidis, and R. Boursier, Josephson Junction through a Thin Ferromagnetic Layer: Negative Coupling, *Phys. Rev. Lett.* **89**, 137007 (2002).
- [53] V. V. Ryazanov, V. A. Oboznov, A. Yu. Rusanov, A. V. Veretennikov, A. A. Golubov, and J. Aarts, Coupling of Two Superconductors Through a Ferromagnet: Evidence for a  $\pi$  Junction, *Phys. Rev. Lett.* **86**, 2427 (2001).
- [54] F. S. Bergeret, A. F. Volkov, and K. B. Efetov, Odd triplet superconductivity and related phenomena in superconductor-ferromagnet structures, *Rev. Mod. Phys.* **77**, 1321 (2005).
- [55] M. Eschrig, J. Kopu, J. C. Cuevas, and G. Schön, Theory of Half-Metal/Superconductor Heterostructures, *Phys. Rev. Lett.* **90**, 137003 (2003).
- [56] K. Halterman, O. T. Valls, and C.-T. Wu, Charge and spin currents in ferromagnetic Josephson junctions *Phys. Rev. B* **92**, 174516 (2015).
- [57] C.-T. Wu and K. Halterman, Spin transport in half-metallic ferromagnet-superconductor junctions, *Phys. Rev. B* **98**, 054518 (2018).
- [58] O. T. Valls, *Superconductor/Ferromagnet Nanostructures*, (World Scientific, Hackensack, NJ, 2022).
- [59] T. Yamashita, A. Kawakami, and H. Terai, NbN-Based Ferromagnetic  $0$  and  $\pi$  Josephson Junctions, *Phys. Rev. Applied* **8**, 054028 (2017).
- [60] T. Yamashita, S. Takahashi, and S. Maekawa, Controllable  $\pi$  junction with magnetic nanostructures, *Phys. Rev. B* **73**, 144517 (2006).
- [61] A. A. Golubov, M. Yu. Kupriyanov, and E. Il'ichev, The current-phase relation in Josephson junctions, *Rev. Mod. Phys.* **76**, 411 (2004).
- [62] S. Kashiwaya and Y. Tanaka, Tunnelling effects on surface bound states in unconventional superconductors, *Rep. Prog. Phys.* **63**, 1641 (2000).
- [63] F. Ando, Y. Miyasaka, T. Li, J. Ishizuka, T. Arakawa, Y. Shiota, T. Moriyama, Y. Yanase, and T. Ono, Observation of superconducting diode effect, *Nature* **574**, 373 (2020).
- [64] Y. Y. Lyu, Ji Jiang, Y.-L. Wang, Z.-L. Xiao, S. Dong, Q.-H. Chen, M. V. Milošević, H. Wang, R. Divan, J. E. Pearson, P. Wu, F. M. Peeters, and W.-K. Kwok, Superconducting diode effect via conformal-mapped nanoholes, *Nat. Commun.* **12**, 2703 (2021).
- [65] C. Baumgartner, L. Fuchs, A. Costa, S. Reinhardt, S. Gronin, G. C. Gardner, T. Lindemann, M. J. Manfra, P. E. Faria Junior, D. Kochan, J. Fabian, N. Paradiso, and C. Strunk, Supercurrent rectification and magneto-chiral effects in symmetric Josephson junctions, *Nat. Nanotechnol.* **17**, 39 (2021).
- [66] K. Halterman, M. Alidoust, R. Smith, and S. Starr, Supercurrent diode effect, spin torques, and robust zero-energy peak in planar half-metallic trilayers, *Phys. Rev. B* **105**, 104508 (2022).
- [67] An early proposal for such diode effect did not require SOC. [68] A superconducting diode effect is also possible with a single S region. [69]
- [68] J. Hu, C. Wu, and Xi Dai, Proposed Design of a Josephson Diode, *Phys. Rev. Lett.* **99**, 067004 (2007).
- [69] N. F. Q. Yuan and L. Fu, Supercurrent diode effect and finite-momentum superconductors, *Proc. Natl. Acad. Sci. USA* **119**, e2119548119 (2022).

- [70] Y. Xu, P.-H. Fu, L. Chen, J.-F. Liu, J. Wang, and H. Xu, Electrically modulated anomalous phase shift in Andreev bound states mediated by chiral Majorana modes, *Phys. Rev. B* **105**, 075409 (2022).
- [71] J. R. Eskilt, M. Amundsen, N. Banerjee, and J. Linder, Long-ranged triplet supercurrent in a single in-plane ferromagnet with spin-orbit coupled contacts to superconductors, *Phys. Rev. B* **100**, 224519 (2019).
- [72] M. Hell, M. Leijnse, and K. Flensberg, Two-Dimensional Platform for Networks of Majorana Bound States, *Phys. Rev. Lett.* **118**, 107701 (2017).
- [73] F. Pientka, A. Keselman, E. Berg, A. Yacoby, A. Stern, and B. I. Halperin, Topological Superconductivity in a Planar Josephson Junction, *Phys. Rev. X* **7**, 021032 (2017).
- [74] T. Yokoyama, M. Eto, and Y. V. Nazarov, Anomalous Josephson effect induced by spin-orbit interaction and Zeeman effect in semiconductor nanowires, *Phys. Rev. B* **89**, 195407 (2014).
- [75] M. Nashaat, A. E. Botha, and Yu. M. Shukrinov, Devil's staircases in the IV characteristics of superconductor/ferromagnet/superconductor Josephson junctions, *Phys. Rev. B* **97**, 224514 (2018).
- [76] D. Massarotti, N. Banerjee, R. Caruso, G. Rotoli, M. G. Blamire, and F. Tafuri, Electrodynamics of Josephson junctions containing strong ferromagnets, *Phys. Rev. B* **98**, 144516 (2018).
- [77] B. Pekerten, J. D. Pakizer, B. Hawn, and A. Matos-Abiague, Anisotropic topological superconductivity in Josephson junctions, *Phys. Rev. B* **105**, 054504 (2022).
- [78] J. D. Pakizer, B. Scharf, and A. Matos-Abiague, Crystalline anisotropic topological superconductivity in planar Josephson junctions, *Phys. Rev. Research* **3**, 013198 (2021).
- [79] B. Scharf, F. Pientka, H. Ren, A. Yacoby, and E. M. Hankiewicz, Tuning topological superconductivity in phase-controlled Josephson junctions with Rashba and Dresselhaus spin-orbit coupling, *Phys. Rev. B* **99**, 214503 (2019).
- [80] T. Zhou, M. C. Dartailh, K. Sardashti, J. E. Han, A. Matos-Abiague, J. Shabani, and I. Žutić, Fusion of Majorana bound states with mini-gate control in two-dimensional systems, *Nat. Commun.* **13**, 1738 (2022).
- [81] P. P. Paudel, T. Cole, B. D. Woods, and T. D. Stanescu, Enhanced topological superconductivity in spatially modulated planar Josephson junctions, *Phys. Rev. B* **104**, 155428 (2021).
- [82] A. Bargerbos, M. Pita-Vidal, R. Žitko, J. Ávila, L. J. Splitthoff, L. Grünhaupt, J. J. Wesdorp, C. K. Andersen, Yu Liu, L. P. Kouwenhoven, R. Aguado, A. Kou, and B. van Heck, Singlet-doublet transitions of a quantum dot Josephson junction detected in a transmon circuit, arXiv:2202.12754.
- [83] M. Hays, V. Fatemi, D. Bouman, J. Cerrillo, S. Diamond, K. Serniak, T. Connolly, P. Krogstrup, J. Nygøard, A. Levy Yeyati, A. Geresdi, and M. H. Devoret, Coherent manipulation of an Andreev spin qubit, *Science* **373**, 6553 (2021).
- [84] L. Casparis, M. R. Connolly, M. Kjaergaard, N. J. Pearson, A. Kringhøj, T. W. Larsen, F. Kuemmeth, T. Wang, C. Thomas, S. Gronin, G. C. Gardner, Superconducting gatemon qubit based on a proximitized two-dimensional electron gas, M. J. Manfra, C. M. Marcus, and K. D. Petersson, *Nat. Nanotechnol.* **13**, 915 (2018).
- [85] T. Yamashita, K. Tanikawa, S. Takahashi, and S. Maekawa, Superconducting Qubit with a Ferromagnetic Josephson Junction, *Phys. Rev. Lett.* **95**, 097001 (2005).
- [86] S. Kawabata, S. Kashiwaya, Y. Asano, Y. Tanaka, and A. A. Golubov, Macroscopic quantum dynamics of  $\pi$  junctions with ferromagnetic insulators, *Phys. Rev. B* **74**, 180502(R) (2006).